

# 1 **A method to predict the uncompleted climate transition** 2 **process**

3 **Pengcheng Yan<sup>1,3</sup>, Guolin Feng<sup>2</sup>, Wei Hou<sup>2</sup>, Ping Yang<sup>3</sup>**

4 [1]{Institute of Arid Meteorology, China Meteorological Administration, Key  
5 Laboratory of Arid Climatic Change and Reducing Disaster of Gansu Province, Key  
6 Laboratory of Arid Climatic Change and Reducing Disaster of China Meteorological  
7 Administration, Lanzhou, China}

8 [2]{Laboratory for Climate Studies, National Climate Center, China Meteorological  
9 Administration, Beijing, China}

10 [3]{China Meteorological Administration Training Center, Beijing, China}

11 [\*]Correspondence to: Wei Hou (houwei@cma.gov.cn)

## 12 **Abstract**

13 Climate change is expressed as a climate system transiting from the initial state to a  
14 new state in a short time. The period between the initial state and the new state is  
15 defined as transition process, which is the key part to connect the two states. By using  
16 a piece-wise function, the transition process is stated approximately (Mudelsee, 2000).  
17 However, the dynamic processes are not included in the piece-wise function. Thus, we  
18 had proposed a method (Yan et al, 2015, 2016) to fit the transition process by using a  
19 continuous function. In this manuscript, this method is developed to predict the  
20 uncompleted transition process based on the dynamic characteristics of the continuous  
21 function. We introduce this prediction method in details and apply it to three ideal  
22 time sequences and the Pacific Decadal Oscillation (PDO). The PDO is a long-lived  
23 El Niño-like pattern of Pacific climate variability (Barnett et al, 1999). A new  
24 quantitative relationship during the transition process has been revealed, and it  
25 explores a nonlinear relationship between the linear trend and the amplitude  
26 (difference) between the initial state and the end state. As the transition process begins,  
27 the initial state and the linear trend are estimated. Then, according to the relationship,  
28 the end state and end moment of the uncompleted transition process are predicted.

# 1     **Keywords**

2           Prediction method; Transition process of abrupt change; System stability; Pacific  
3     Decadal Oscillation

## 4     **1. Introduction**

5           A system transiting from one stable state to another in a short period is called  
6     abrupt change (Charney and DeVore, 1979; Lorenz, 1963, 1979). The abrupt change  
7     system has two or more states (Goldblatt et al, 2006; Alexander et al, 2012), the  
8     system swings between these states that are also called equilibrium states in physics.  
9     This phenomena is verified in many fields including biology (Nozaki, 2001), ecology  
10    (Osterkamp et al, 2001), climatology (Thom, 1972; Overpeck and Cole, 2006; Yang et  
11    al, 2013a, 2013b), brain science (Sherman et al, 1981), etc. The cusp catastrophe has  
12    been detected in climatology widely. Many researches studied the characteristics and  
13    early warning signals of the cusp catastrophe ( Lenton, 2012; Pierini, 2012; Livina et  
14    al, 2012). The latest observed climate change event was global warming hiatus  
15    (Amaya et al, 2018; Kosaka and Xie, 2013; Yang et al, 2017). In Thom’s  
16    research(1972), seven different kinds of abrupt changes were mentioned. Over the last  
17    several decades, many methods have been proposed to identify different kinds of  
18    abrupt change (Li et al, 1996), such as Moving T-Test, Cramer’s (Wei, 1999),  
19    Mann-Kendall (MK, Goossens and Berger, 1986), Fisher (Cabezas and Fath, 2002),  
20    etc. It is noticed that most abrupt change detection methods suggest that the abrupt  
21    change is around a turning point. The significant difference between the average  
22    values of the two sequences on both two sides of the turning point is defined as the  
23    index to measure the abrupt change. It is difficult for these kinds of methods to detect  
24    the transition period of the abrupt change, and it is difficult to identify the abrupt  
25    change that occurs at the end of sequence.

26           Mudelsee (2000) studied the abrupt change of a time sequence and illustrated  
27    that abrupt change has a duration, which can be quantitatively described with a  
28    piece-wise (ramp) function. We developed the detection method by using a

1 continuous function to replace the ramp function( Yan et al, 2014, 2015). The new  
2 method can confine the beginning and ending points of abrupt change and  
3 quantitatively describes the process of abrupt climate change, and three parameters  
4 are introduced. A quantitative relationship among the parameters is revealed (Yan et al,  
5 2015). The relationship could be used to predict the end moment (state) if the system  
6 had left the original state but not yet reached to the new state, which is defined as an  
7 uncompleted transition process.

8 In this manuscript, three ideal time sequences are tested to study the prediction  
9 method. The prediction method is also applied to study the climate transition process  
10 of the PDO, which is an important signal that reveals climatic variability on the  
11 decadal timescale (Mantua et al, 1997; Barnett et al, 1999; Zhang et al, 1997; Yang et  
12 al, 2004). Previous studies (Lu et al, 2013; Trenberth and Hurrell, 1994) have  
13 indicated that there are many abrupt changes in the PDO over the past 100 years.  
14 Most researches mentioned the climate changes happened in the 1940s and 1970s.  
15 During the 1940s, the PDO transited from a high state to a low state, while during the  
16 1970s, it did the opposite. All of these changes and their processes had been studied in  
17 our previous research (Yan et al, 2015 2016). The climate transition processes were  
18 explored clearly. However, we still can not know when the transition processes finish  
19 their increasing or decreasing to a stable state if the transition process has begun. We  
20 develop a new method to predict the end state and the end moment of a transition  
21 process based on the quantitative relationship.

## 22 **2. Methods**

23 It is necessary to describe the transition process quantitatively before the  
24 prediction of the uncompleted climate transition process. The detection method by  
25 using the logistic model to obtain a transition process is introduced in section 2.1. On  
26 the basis of the detection method, the prediction method for studying the uncompleted  
27 transition process is further developed in section 2.2.

## 2.1 The detection method of transition process

The real time sequence changes abruptly as shown in figure 1a, and the system jumps to a high state in point  $C$ . If the period around point  $C$  is observed on a shorter time scale (as shown figure 1b), a transition period is obtained, and it is a part of the original time sequence. In fact, many abrupt changes could be considered to be a transition period with a more detailed view. The transition period was expressed with a ramp function in Mudelsee's research (2000) as shown in figure 1c, and the time sequence is divided into three segments, including two equilibrium states and one increasing state. The ramp function is as follows:

$$x_t = \begin{cases} x_1 & t \leq t_1 \\ x_1 + (t - t_1)(x_2 - x_1)/(t_2 - t_1) & t_1 < t \leq t_2 \\ x_2 & t > t_2 \end{cases}, \quad (1)$$

where  $t$  represents time, and  $x_t$  represents the system state. Before  $t_1$  and after  $t_2$ , the system stays in the two equilibrium states  $x_1$ , and  $x_2$ . Between  $t_1$  and  $t_2$ , the system's states are a straight line. It is noted that the climate system should be smooth and continuous; it is even the sampling sequence that makes it is discrete. We used a continuous function to express this transition period approximately, and we also created a novel method to detect the transition period (Yan et al, 2015). As shown in figure 1d, the transition process is consistent with the continuous evolution of the logistic model, which was created to describe the evolution of population model(May, 1976). The modified logistic model with two changeable equilibrium states is expressed as equation (2), which  $x$  represents variable of system state,

$$\frac{dx}{dt} = k(x - u)(v - x). \quad (2)$$

Parameters  $u$  and  $v$  represent the two equilibrium states respectively. Parameter  $u$  represents initial state, and parameter  $v$  represents end state. Parameter  $k$  represents the switching between different states, and it is defined as the instability parameter. As shown in figure 2a, parameters  $u$  and  $v$  being fixed, and setting  $k$  as 0.4 ( the dash gray line), the system increasing to the new state costs a shorter time than that setting  $k$  as

1 0.3 (the black line). It is noted that if  $k < 0$  ( as  $v=1.0$ ,  $u=2.0$  and  $k=-0.4$  ), the system  
 2 decreases from state 2.0 to state 1.0 as the gray line. This states that if the absolute  
 3 value of  $k$  is relatively large, the shorter the transition time of the system, that is, the  
 4 more unstable(Yan et al, 2016). If parameter  $k$  is set large enough, the system  
 5 collapses and becomes chaotic as shown in figure 2b.

6 In equation (2), the first derivative of state variable to time is given, and it is  
 7 regarded as velocity. The acceleration  $\frac{d^2x}{dt^2}$  of state variable is expressed as the  
 8 derivative of velocity to time, as shown in equation (3). The acceleration of the  
 9 system is from the external force  $f(x)$ , which is expressed as  $f(x) = m \frac{d^2x}{dt^2}$  .

10 Assuming that the coefficient  $m$  is 1, the generalized potential energy (Benzi et al,  
 11 1982) is expressed as the integral of the generalized force to the state, as shown in  
 12 equation(4),

$$\begin{aligned}
 f(x) &= \frac{d^2x}{dt^2} = \frac{d[k(x-u)(v-x)]}{dt} = \frac{d[-kx^2 + k(u+v)x - kuv]}{dt} \\
 &= [-2kx + k(v+u)] \frac{dx}{dt} = 2k^2[x - (u+v)/2](x-u)(x-v) , \\
 &= k^2[2x^3 - 2(u+v)x^2 + (u^2 + v^2 + 4uv)x - (u+v)uv]
 \end{aligned} \tag{3}$$

$$\begin{aligned}
 V(x) &= -\int_0^x f(x)dx = -\int_0^x k^2[2x^3 - 2(u+v)x^2 + (u^2 + v^2 + 4uv)x - (u+v)uv]dx \\
 &= \frac{k^2}{2}[x^4 - 2(u+v)x^3 + (u^2 + v^2 + 4uv)x^2 - 2(u+v)uvx]
 \end{aligned} \tag{4}$$

15 According to Thom's theory (1972), the generalized potential energy of the system  
 16 described by a quartic function would exhibit cusp catastrophe in which the system  
 17 jumps from one state to a new state abruptly.

18 In figure 2c, the potential energy of equation (4) is verified to have two states  
 19 with the lowest energy, and both of them are stable. This bistable structure is common  
 20 in the climate system (Goldblatt et al, 2006). Therefore, equation (2) can be used to  
 21 describe the abrupt change system, and the parameters of equation (2) represent  
 22 different key factors of the transition period during abrupt change. In order to obtain  
 23 the values of parameters, the time sequence is divided into three segments. The first

1 and the third segment represent the two equilibrium states, while the second segment  
 2 represents the transition process. During the transition process, we define a new  
 3 parameter  $h$  to represent the ratio of system state change to time, and it is called linear  
 4 trend. As equation (5), the linear trend  $h$  can be expressed by two points on the curve  
 5 approximately, where the two points are  $A(x_a, t_a)$  and  $B(x_b, t_b)$  which are displayed in  
 6 figure 2d,

$$7 \quad h = \frac{x_a - x_b}{t_a - t_b} \quad (5)$$

8 In equation (6), the values of parameters  $v$  and  $u$  are calculated. The value of  
 9 parameter  $h$  can be calculated by the regression method (Huang, 1990; Yang et al,  
 10 2013a) based on the time sequence of the second segment, where  $i, x_i$  denote the time  
 11 and the system state, and  $\bar{i}, \bar{x}_i$  are their averages respectively. Variables  $n_1, n_2, n_3$   
 12 represent the lengths of the first, the second and the third segment respectively.

$$13 \quad \begin{cases} v = \sum_{i=1}^{n_1} x_i / n_1 \\ u = \sum_{i=n_1+n_2+1}^n x_i / n_3 \\ h = \sum_{i=n_1+1}^{n_1+n_2} \bar{i} \cdot \bar{x}_i / \sum_{i=n_1+1}^{n_1+n_2} \bar{i}^2 \end{cases} \quad (6)$$

14 The points  $A(x_a, t_a)$  and  $B(x_b, t_b)$  are also on the curve, thus we are going to  
 15 calculate the solution of equation (2). The equation 2 is rewritten to be equation 7 and  
 16 both sides of the equation 7 are integrated as equation (8),

$$17 \quad dt = \frac{dx}{k(x-u)(v-x)} \quad (7)$$

$$18 \quad \begin{aligned} \int_{t_0}^t dt &= \int_{x_0}^x \frac{1}{k(u-v)} \left( \frac{1}{x-u} - \frac{1}{x-v} \right) dx \\ \Rightarrow t \Big|_{t_0}^t &= \frac{1}{k(u-v)} \ln \left( \frac{x-v}{x-u} \right) \Big|_{x_0}^x \\ \Rightarrow t &= \frac{1}{k(u-v)} \ln \left( \frac{x-v}{x-u} \cdot \frac{x_0-u}{x_0-v} \right) + t_0, \end{aligned} \quad (8)$$

1 Where the variables  $t_0$  and  $x_0$  represent the initial time and the initial state  
 2 respectively. The transition process has been assuming to be linear, thus we define  
 3 location parameters  $\alpha$  and  $\beta$ ,  $\alpha = \frac{x_a - v}{u - v}$ ,  $\beta = \frac{x_b - v}{u - v}$ , and  $x_a$ ,  $x_b$  are expressed as  
 4 follows,

$$5 \begin{cases} x_a = \alpha(u - v) + v \\ x_b = \beta(u - v) + v \end{cases} \quad (9)$$

6 Substituting equation (8) and equation (9) into equation (7), we have:

$$7 \begin{aligned} h &= \frac{x_b - x_a}{t_b - t_a} = \frac{(\beta - \alpha)(u - v)}{\frac{1}{k(u - v)} \left( \ln\left(\frac{x_b - v}{x_b - u}\right) - \ln\left(\frac{x_a - v}{x_a - u}\right) \right)} \\ &= k(u - v)^2 \frac{(\beta - \alpha)}{\ln \frac{\beta(\alpha - 1)}{\alpha(\beta - 1)}} \end{aligned} \quad (10)$$

8 It is noted that the rightmost part is only related to parameters  $\alpha$  and  $\beta$ , then let it  
 9 be  $\chi$ . Then, the relationship of equation (10) is rewritten as equation (11),

$$10 \quad h = k(u - v)^2 \chi \quad (11)$$

11 The difference between the initial state  $v$  and the end state  $u$ ,  $u - v$ , is called as the  
 12 amplitude of change. In order to determine the value of parameter  $\chi$ , the relationship  
 13 among  $\chi$ ,  $\alpha$ ,  $\beta$  is displayed in figure 3b. The dash line in figure 3a is the profile of the  
 14 diagonal in figure 3b, which represents that the sum of  $\alpha$  and  $\beta$  is 1. Parameter  $\chi$   
 15 changes little when the location parameter varies in a certain range as marked with  
 16 warm color in figure 3b. It means that the closer the points ( $A$  and  $B$ ) are to the  
 17 middle point, the more significant the linear feature is. Then, the process between  
 18 point  $A$  and point  $B$  can represent the whole transition process as shown in figure 3c.  
 19 It is noted that the transition process is symmetrical about the middle point  
 20 approximately. Thus, we assume that point  $A$  and point  $B$  are symmetrical about the  
 21 middle point, and the sum of  $\alpha$  and  $\beta$  is 1. The change of parameter  $\chi$  is only related to  
 22 parameter  $\alpha$  (or parameter  $\beta$ ), as shown in the diagonals in figure 3b (also in figure 3a).  
 23 Parameter  $\chi$  changes little when parameter  $\alpha$  is about 0.2 or larger. In figure 3c, three  
 24 different situations are carried out to study the influence of parameter  $\alpha$  on parameter

1  $\chi$ . In each situation, points ( $A$  and  $B$ ) are set to be different positions, and their  
2 parameters were calculated respectively in table 1. The parameters  $\alpha$  are set as 0.20,  
3 0.25, 0.15 respectively in three different situations marked with S1, S2 and S3. For S2  
4 and S3, both of the percentages of  $\alpha$  changing to S1 are 25%, while the percentages of  
5  $\chi$  changing are only 5.15% and 6.76% respectively, which means the percentage  
6 change of  $\chi$  is much less than  $\alpha$ . In addition, linear trends of these three ideal models  
7 are calculated according to the points and by regression method which are marked as  
8  $h_0$  in table 1. The linear trends are also calculated by the values of point  $A$  and point  $B$   
9 with Eq(5) which are marked as  $h$  in table 1. It is noted that although the positions of  
10 points are different, the trend obtained according to the points is almost the same as  
11 that obtained by regression method. The error percentages are 2.36%, 2.25%, 1.38%  
12 respectively, which means that we don't have to know the exactly positions of point  $A$   
13 and  $B$  (the values of parameters  $\alpha$  and  $\beta$ ). We can approximate the value of  $\chi$ . Thus, in  
14 the following sections parameter  $\alpha$  is set as 0.2, and parameter  $\chi$  is 0.2164.

## 15 **2.2 The prediction method of transition process**

16 Equation (11) shows the quantitative relationship among linear trend, instability  
17 parameter, and amplitude of change. There is a linear relationship between linear  
18 trend and instability parameter; and there is a quadratic function relationship between  
19 linear trend and amplitude of change. We revealed this quantitative relationship  
20 based on sea surface temperature(Yan et al, 2016). According to this relationship, we  
21 are going to develop a new method to predict the transition process which has not  
22 been completed. A brief description about the new method is stated with the schematic  
23 diagram in figure 4. The red line represents the period which has been experienced,  
24 while the gray line represents the period which has not been experienced. Based on  
25 the system states which are far away from the original state, a quasi linear extension  
26 of the transition process is established as dash line. Then the parameters  $v$  and  $h$  are  
27 obtained by equation (6). The instability parameter  $k$  represents the stability of abrupt  
28 changes of the system, which means that it's related to the system. Its threshold can be  
29 estimated by history data. The parameter  $u$  is predicted by equation (11), and the end



1 moment can be determined according to the definition of linear trend  $h$ .

2 In order to test the prediction method, an ideal time sequence is constructed by  
3 using equation (12), which is the sum of the logistic model and random numbers,  
4 where  $\eta_t$  represents the random number,

$$5 \begin{cases} x_t = x_{t-1} + kt(x_t - u)(v - x_t) \\ x'_t = x_t + \eta_t \end{cases} \quad (12)$$

6 As shown in figure 5, An entire time sequence with 500 moments is shown in  
7 figure 5a and three other time sequences with different lengths are shown in figures  
8 5b, 5c and 5d respectively. The parameters  $v$ ,  $u$  and  $k$  of the logistic model are set as  
9 -1.0, 2.0, 0.1, for the ideal time sequence, and the random number is limited in 0-1.  
10 The parameters  $v$ ,  $h$  are obtained by regression method before making prediction. It  
11 has to be noted that in this ideal time sequence there is just one abrupt change, which  
12 means that we have no way to obtain the value of the parameter  $k$  by counting other  
13 abrupt changes. Thus parameter  $k$  is given directly, and the prediction of the end state  
14 ( moment) is drawn in figure 5b, 5c and 5d. For the entire time sequence, there are  
15 500 moments as shown in figure 5a. In figure 5b, only 240 moments are given, and  
16 the other moments are unknown. Then, we obtain parameters  $v$  and  $h$  by regression  
17 method. The parameter  $u$  is calculated with equation (6). The blue line represents the  
18 prediction result. The transition process would be ended in moment 342 with the end  
19 state value 2.92. In figure 5c, the end moment and end state are predicted to be 356  
20 and 2.65 respectively when the time sequence is given 250 moments. In figure 5d, the  
21 time sequence is given 260 moments. The end moment and end state are predicted to  
22 be 359 and 2.58 respectively. The prediction end moment and the prediction end state  
23 are basically consistent with the original time sequences. However, the average  
24 absolute prediction errors of the three time sequences are 0.37, 0.27 and 0.26  
25 respectively. When the length of the sequence is 240, the prediction state is  
26 overestimated, and the average absolute prediction error is 0.37. With the length of the  
27 system experienced expanding, the prediction error decreases. The prediction states  
28 are very close to the original states when the length is 260. Therefore, in the actual  
29 prediction, we hope that the transition process has been experienced for a long enough

1 time, which will help to predict accurately.

## 2 **3. Results**

3 In order to test the validity of this prediction method in a real climate system, we  
4 apply this method to predict the uncompleted transition process of the PDO. The PDO  
5 index data used is from website of the University of Washington  
6 (<http://research.jisao.washington.edu/pdo/>). The time period from January of 1900 to  
7 November of 2015 is studied as the training data, and the time period from December  
8 of 2015 to April of 2017 is used as the test data. During the following research, a  
9 transition process starting from 2011 is studied. According to the prediction method,  
10 several parameters have to be determined in advance. We first determine parameter  $k$ .

### 11 **3.1 Threshold of parameter $k$**

12 Parameter  $k$  characterizes the stability of the system during climate change,  
13 which means that we can estimate the value of parameter  $k$  by counting all abrupt  
14 changes of the PDO index. The histogram in Figure 6a shows the PDO time sequence  
15 from January of 1900 to November of 2015, and it shows that the PDO went through  
16 several transition processes. The green dots in Figure 6a are parameter  $k$  when the  
17 sub-sequence length takes 20 years. In the early 1940s and late 1970s, there are two  
18 main transitions of the PDO. The absolute value of the parameter  $k$  is large, which  
19 means that the system is much more unstable during this two transition processes. In  
20 the 1940s, the PDO transits from a positive phase to a negative phase, and  $k < 0$ ,  
21 whereas the situation in the 1970s is the opposite. Figure 6b shows more  $k$  values  
22 corresponding to the different sub-sequence lengths (as indicated by Y-axis, the  
23 variation range of the sub-sequence is 15-60 years, with an interval of 1 year). The  
24 X-axis represents the start moment, and the locations of the dots indicate the start  
25 moments for the corresponding sub-sequence lengths. In particular, the blue dots  
26 represent that parameter  $k$  is negative, and the red dots represent that it is positive.  
27 There are more dots when the sub-sequence is short. This is because when the length

1 of sub-sequence is short, the amplitude is also often small, which leads that more  
2 transition processes are detected. When the length of the sub-sequence reaches or  
3 exceeds 50 years, the transition processes mainly begin in the 1940s and 1970s. Such  
4 climate changes are also investigated in the previous research (Shi et al, 2014). The  
5 transition processes in these two periods correspond to large  $k$  values, which means  
6 that these two transition processes are more unstable than others. The small figure in  
7 figure 7 (a) shows that the  $k$  values (marked with green dots) are more than 100 during  
8 1960~1970 when the length of sub-sequence is 20 years. The frequencies of  
9 parameter  $k$  values when the length of sub-sequence are 10, 20, 20, 40, 50, and 60  
10 years respectively are displayed in figure 7. It is noted that some of the values of  
11 parameter  $k$  are so large that their frequencies are almost zero which are not necessary  
12 to be counted. The frequencies of  $k$  values which belongs to -10 to 10 are shown in  
13 figure 7. By considering the frequency which is bigger than 5% as a peak, there is  
14 only one peak when the length of sub-sequence is 10 years. Most of the  $k$  values are  
15 concentrated around zero, which means that the transition processes detected are  
16 stable. For the situations which the lengths of sub-sequences are 20 and 30 years,  
17 there is one mainly peak, and it is near zero. When the lengths of sub-sequences are  
18 more than 30 years, there are two mainly peaks. One is near zero, and another is much  
19 less than zero. It states that the much more unstable transition processes are detected  
20 when the lengths of sub-sequences are large. From the perspective of the  $k$  threshold  
21 values, the  $k$  values in the range of (-10, 10) accounts for 63.90%, 70.64%, 77.00%,  
22 90.05%, 93.69%, and 89.90% of all  $k$  values for that the lengths of sub-sequences are  
23 10, 20, 30, 40, 50, 60 years respectively. They are 55.64%, 67.52%, 73.99%, 83.45%,  
24 85.46%, 84.82% for the range of (-5, 5) and 35.64%, 62.22%, 59.36%, 68.28%,  
25 66.25%, 47.55% for the range of (-2, 2). In the following studies, the  $k$  values are  
26 mainly considered to be in the range of (-2, 2).

### 27 **3.2 Values of the initial state $v$ and linear trend $h$**

28 We use the method proposed in section 2.2 to analyze the transition processes of

1 the PDO. With different lengths of sub-sequences, three climate changes are detected  
2 to start from 1976, 2007 and 2011 respectively. In figure 8, the transition processes  
3 starting from 2007 and 2011 are shown, while the transition process starting from  
4 1976 has not been shown. In table 2, parameters  $v$  and  $h$  are obtained by regression  
5 method for the transition processes starting from 2007 and 2011. When the length of  
6 sub-sequence is 10 years or 20 years, only the transition process starting from 2011 is  
7 detected as shown in figure 8a and figure 8b. The parameter  $v$  is calculated with the  
8 sequence before 2011. Then, the linear trend parameter  $h$  is calculated with the  
9 segment after 2011. For the transition process starting from 2011, the values of initial  
10 state were detected to be -0.45 and -0.03 when the length of sub-sequence is 10 years  
11 or 20 years respectively, and both the linear trends are 1.054/month. When the lengths  
12 of sub-sequences are set as 30 and 40 years, the transition process began in 2007 as  
13 shown in figure 8c and figure 8d, and the values of initial state are 0.36 and 0.41,  
14 respectively, with an linear trend of 0.227/month. When we detect the transition  
15 process in a sub-sequence, the percentile threshold method (Huang, 1990) is used.  
16 Then, a transition process in the sub-sequence is detected (Yan et al, 2015, 2016). The  
17 change with the largest amplitude will be detected. The start moment of the transition  
18 process is identified to be 2011 as shown in table 2.

19 In figure 8, it is noted that the PDO time sequence is leaving the stable state from  
20 the start moment. The transition process occurs over a period of time, which is called  
21 the transition process. When the transition process has not finished, it appears to be  
22 increasing part. In order to detect whether there are other transition processes, we  
23 change the length of the sub-sequences to yearly intervals. That is, the sub-sequence  
24 length is set as 10, 11, 12, ..., up to 60 years. Then, the initial state  $v$  and the linear  
25 trend  $h$  of these transition processes are obtained as shown in figure 9. When the  
26 sub-sequence length is set less than approximately 40 years, the transition processes  
27 are detected only twice. One began in 2007, and the other began in 2011. The value of  
28 parameter  $h$  is unchangeable nearly for each transition process, while the value of  
29 parameter  $v$  is changing when the length of sub-sequence is different. In particular, the  
30 transition process starting from 2007 is detected for the sub-sequences of about 30-40

1 years, and the value of parameter  $\nu$  is in the range of (0.28, 0.45). The transition  
2 process starting from 2011 is detected for the sub-sequences of about 10-30 years, and  
3 the value of parameter  $\nu$  increases as the length of the sub-sequence increases,  
4 whereas the variation range of parameter  $\nu$  is (-0.48, 0.12), which is significantly  
5 different from the situation of the transition process starting from 2007.

### 6 **3.3 Prediction of the uncompleted transition process beginning in** 7 **2011**

8 After the threshold ranges for parameters  $k$ ,  $\nu$ , and  $h$  are determined, according to  
9 the quantitative relationship, we can calculate the end state and the end moment of the  
10 transition process. Using the transition process in 2011 as an example, we study the  
11 ending state and end moment for the PDO index transition process. According to the  
12 research results that are presented in Sections 3.1 and 3.2, the parameter is  
13  $h=1.054/\text{month}$  in this transition process, and the threshold range of parameter  $k$  is  
14 determined to be (0, 2). The range of parameter  $\nu$  is determined to be (-0.48, 0.12),  
15 and the variation situation of parameter  $u$  and end moment with parameters  $k$  and  $\nu$   
16 are shown in Figure 10. The results indicate that the threshold range of parameter  $u$   
17 for the ending state is (1, 7), and the time range of the ending moment is (2013, 2017).  
18 According to the probability of parameter  $k$ , the end moment of this transition process  
19 is about 2015, and after that time, the sequence stops to increase, approaching to a  
20 stable state with value of 1.6.

21 In figure 11, a sketch map is displayed to briefly explain how the prediction  
22 method works. The PDO time sequence is displayed as a black line. The period during  
23 2006~2011 is detected as the initial state, and a transition process is increasing from  
24 this initial state. It is not able to be known whether the increasing process has been  
25 completed or not. Based on the linear regression method, the initial state and the  
26 linear trend are obtained and shown as purple dash lines. Then by the method  
27 proposed in section 2.2, all possible end states of this transition process are obtained  
28 with equation (9) as shown in figure 10, and the most likely end state is marked as a

1 green dash line.. Unlike the uncompleted transition process of ideal experiment, the  
2 transition process has completed in about 2015 since we detected the PDO change in  
3 2016. This transition process started from 2011 and ends in 2015. The initial moment  
4 and the end moment are marked as black dash lines. However, we are still not sure  
5 whether the PDO finish this transition process completely or not for it it appears at the  
6 end of the sequence. Many statistical methods are not accurate for the detecting both  
7 ends of the sequence. Thus, the real PDO sequence during 2016~2017 is added to the  
8 end of the PDO time sequence. The PDO value from 2015 to 2017 is almost  
9 unchanged, which is consistent with the predicted result.

#### 10 **4. Conclusion and discussion**

11 A novel method had been proposed to identify the transition process of climate  
12 change in our previous research. By defining initial state parameter  $v$ , linear trend  
13 parameter  $h$ , end state parameter  $u$ , and instability parameter  $k$ , a quantitative  
14 relationship among these parameters was revealed. Based on the relationship, we  
15 develop a method to study uncompleted transition processes. The method is applied to  
16 predict ideal time sequences and the PDO time sequence. In the ideal experiments,  
17 three different time sequences with different length are constructed. Based on the  
18 initial state and the linear trend which the system had experienced, and the given  
19 parameter, the end state and end moment of the transition process are predicted. The  
20 prediction result does match the ideal time sequence well. For the PDO time sequence,  
21 a transition process beginning in 2011 was taken to test the prediction method. The  
22 end moment of this transition process is predicted to be 2015. which is consistent with  
23 the real time sequence.

24 In this prediction method, the quantitative relationship among the parameters  
25 characterizing the transition process is vital. According to the segment of the  
26 transition process which has been occurred, we determine the parameters and predict  
27 the end moment and the end state. In fact, this is also a extrapolation method. It is  
28 noted that the uncompleted climate change we studied is closed to the end of the

1 sequence. Due to the lack of enough data, it is difficult to study the end of time  
2 sequence by using other statistical methods.

### 3 **Acknowledgements**

4 We thank two anonymous reviewers for their valuable suggestions. This study  
5 was jointly sponsored by National Key Research and Development Program of China  
6 (Grant No. 2018YFE0109600), National Natural Science Foundation of China (Grant  
7 Nos. 41675092, 41775078, 41875096), Northwest Regional Numerical Forecasting  
8 Innovation Team (GSQXCXTD-2020-02), Meteorological scientific research project  
9 of Gansu Meteorological Bureau (MS201914).

### 10 **References**

- 11 Alexander R, Reinhard C, Andrey G. Multistability and critical thresholds of the Greenland ice sheet. *Nature*  
12 *Climate Change* 2012; 429-432
- 13 Amaya D, Siler N, Xie S, Miller A. The interplay of internal and forced modes of Hadley Cell expansion: lessons  
14 from the global warming hiatus. *Climate Dyn* 2018; 51, 305–319, doi:10.1007/s00382-017-3921-5
- 15 Barnett TP, Pierce DW, Latif M. et al. Interdecadal interactions between the tropics and midlatitudes in the Pacific  
16 basin. *Geophys. Res. Lett.*,1999, 26: 615-618.
- 17 Benzi R, Parisi G, Sutera A, et al. Stochastic resonance in climatic change. *Tellus*. 1982, 34: 10–16
- 18 Cabezas H, Fath BD. Towards a theory of sustainable systems. *Fluid Phase Equilibria* 2002; 194–197 3,  
19 doi:10.1016/S0378-3812 (01)00677-X
- 20 Charney JG, DeVore JG. Multiple flow equilibria in the atmosphere and blocking, *J. Atmos. Sci* 1979; 36,  
21 1205–1216, doi: 10.1175/1520-0469 (1979)0362.0.CO;2
- 22 Goldblatt C, Lenton TM, Watson AJ. Bistability of atmospheric oxygen and the Great Oxidation. *Nature* 2006;  
23 443:683-686, doi: 10.1038/nature05169
- 24 Goossens C, Berger A. Annual and Seasonal Climatic Variations over the Northern Hemisphere and Europe during  
25 the Last Century. *Annals of Geophysics* 1986; 4: 385, doi: 10.1016/0040-1951 (86)90317-3
- 26 Huang JY. *Meteorological Statistical Analysis and Prediction*, Beijing: China Meteorological Press 1990; 28–30
- 27 Kosaka Y, Xie SP. Recent global-warming hiatus tied to equatorial Pacific surface cooling. *Nature* 2013; 501:  
28 403–407, doi: 10.1038/nature12534
- 29 Li JP, Chou JF, Shi JE. Complete detection and types of abrupt climatic change. *Journal of Beijing Meteorological*  
30 *college* 1996; 1:7-12

- 1 Lenton TM . Arctic Climate Tipping Points. *Ambio*, 2012, 41(1):10-22.
- 2 Liu TZ, Rong PPg, Liu SD, Zheng ZG, Liu SK. Wavelet analysis of climate jump. *Acta Geophysica Sinica* 1995;  
3 38 (2):158-162
- 4 Livina VN , Ditlevsen PD , Lenton TM . An independent test of methods of detecting system states and  
5 bifurcations in time-series data. *Physica A Statal Mechanics & Its Applications*, 2012, 391(3):485-496.
- 6 Lorenz EN. Deterministic nonperiodoc flow. *J. Atmos. Sci* 1963; 20:130, doi: 10.1175/1520-0469  
7 (1963)020<0130:DNF>2.0.CO;2
- 8 Lorenz EN. Nondeterministic theories of climatic change. *Quaternary Research* 1976; 6 (4):495-506, doi:  
9 10.1016/0033-5894 (76)90022-3
- 10 Lu CH, Guan ZY, Li YH, Bai YY. Interdecadal linkages between Pacific decadal oscillation and interhemispheric  
11 oscillation and their possible connections with East Asian Monsoon. *Chinese J. Geophys* 2013; 56 (4):1084-1094,  
12 doi: 10.1002/cjg2.20012
- 13 Mantua NJ, Hare S, Zhang Y, John W, Robert F. A Pacific Interdecadal Climate Oscillation with Impacts on  
14 Salmon Production PDO. *Bull.amer.meteor.soc* 1997; 78 (6):1069-1079, doi; 10.1175/1520-0477  
15 (1997)078<1069:APICOW>2.0.CO;2
- 16 May RM. Simple mathematical models with very complicated dynamics. *Nature* 1976, 261:459–467, doi:  
17 10.1201/9780203734636-5
- 18 Mudelsee M. Ramp function regression: a tool for quantifying climate Transitions, *Comput. Geosci* 2000,  
19 26:293–307, 10.1016/s0098-3004 (99)00141-7
- 20 Nozaki K. Abrupt change in primary productivity in a littoral zone of Lake Biwa with the development of a  
21 filamentous green-algal community. *Freshwater Biology*, 2001, 46(5):587-602.
- 22 Newman M, Alexander MA, Ault TR, Cobb KM. The Pacific Decadal Oscillation, Revisited. *J. Climate* 2016; 29:  
23 4399–4427, doi: 10.1175/JCLI-D-15-0508.1
- 24 Osterkamp S, Kraft D, Schirmer M. Climate change and the ecology of the Weser estuary region: Assessing the  
25 impact of an abrupt change in climate. *Climate Research*, 2001, 18(1):97-104.
- 26 Overpeck JT, Cole JE. Abrupt change in earth’s climate system. *Annu. Rev. Environ. Resour*, 2006; 31:1-31 doi:  
27 10.1146/annurev.energy.30.050504.144308
- 28 Pierini S. Stochastic tipping points in climate dynamics . *Physical review E*, 2012: 85, 027101
- 29 Sherman DG, Hart RG, Easton JD. Abrupt change in head position and cerebral infarction. *Stroke* 1981; 12 (1):2,  
30 doi: 10.1161/01.STR.12.1.2
- 31 Shi WJ, Tao FL, Liu JY, Xu XL, Kuang WH, Dong JW, Shi XL. Has climate change driven spatio-temporal  
32 changes of cropland in northern China since the 1970s? *Climatic Change* 2014; 124:163-177, doi:  
33 10.1007/s10584-014-1088-1
- 34 Thom R. *Stability Structural and Morphogenesis*. Sichuan:Sichuan Education Press, 1972
- 35 Trenberth KE, Hurrell JW. Decadal atmosphere-ocean variations in the Pacific. *Clim. Dyn* 1994; 9:303-319, doi:  
36 10.1007/BF00204745



1 Wei FY. Modern Climatic Statistical Diagnosis and Forecasting Technology, Beijing: China Meteorological Press,  
2 1999

3 Yan PC, Feng GL, Hou W, Wu H Statistical characteristics on decadal abrupt change process of time sequence in  
4 500 hPa temperature field. Chinese Journal of Atmospheric Sciences 2014; 38 (5): 861–873

5 Yan PC, Feng GL, Hou W. A novel method for analyzing the process of abrupt climate change. Nonlinear  
6 Processes in Geophysics 2015; 22:249-258, doi: 10.5194/npg-22-249-2015

7 Yan PC, Hou W, Feng GL Transition process of abrupt climate change based on global sea surface temperature  
8 over the past century, Nonlinear Processes in Geophysics 2016; 23:115–126, doi:10.5194/npg-23-115-2016

9 Yang XQ, Zhu YM, Xie Q, Ren XJ. Advances in studies of Pacific Decadal Oscillation. Chinese Journal of  
10 Atmospheric Sciences 2004; 28 (6):979-992

11 Yang P, Xiao ZN, Yang J, et al. Characteristics of clustering extreme drought events in China during 1961–2010.  
12 Acta Meteorologica Sinica, 2013a, 27(2):186-198.

13 Yang P, Ren GY, Liu W. Spatial and temporal characteristics of Beijing urban heat island intensity. Journal of  
14 applied meteorology and climatology, 2013b, 52(8):1803-1816.

15 Yang P, Ren GY, Yan PC. Evidence for a strong association of short-duration intense rainfall with urbanization in  
16 the Beijing urban area. Journal of Climate, 2017, 30(15):5851-5870.

17 Zhang YJ, Wallace M, Battisti DS. ENSO-like interdecadal variability :1900-93. J .Climate 1997; 10:1004-1020,  
18 doi: 10.1175/1520-0442 (1997)010<1004:ELIV>2.0.CO;2

19

20

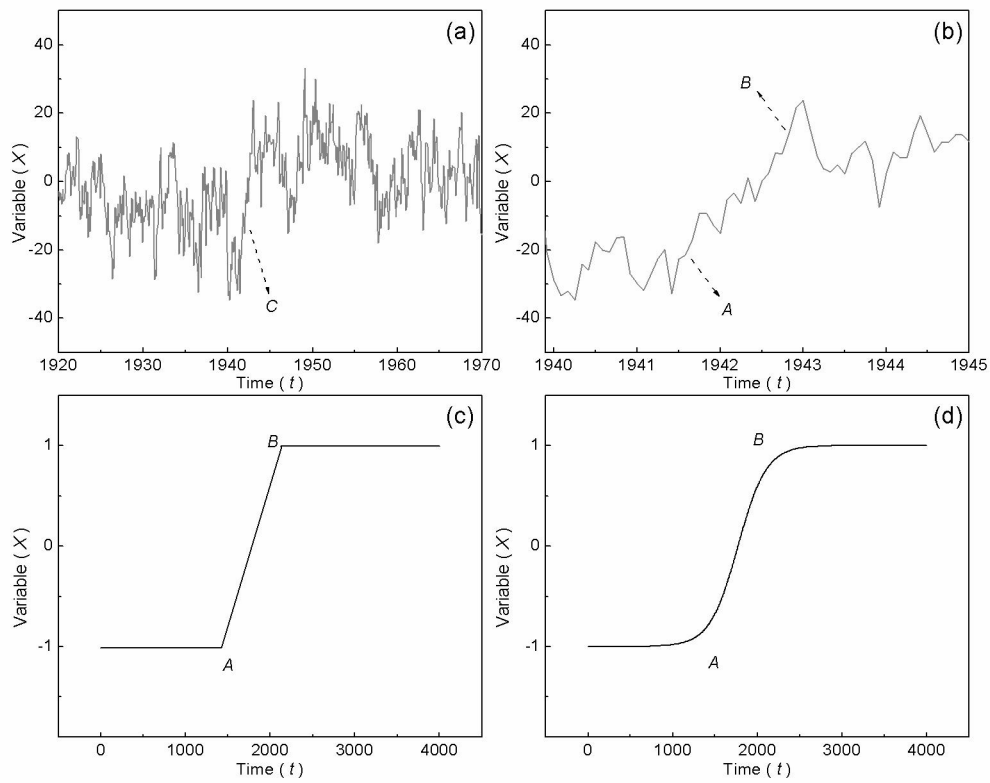
1 Table1. The parameters of ideal models

Situations	$\alpha$	$\chi$	$h_0$	$h$	$ h_0-h /h$
S1	0.20	21.64E-2	12.99E-4	12.69E-4	2.36%
S2	0.25	22.76E-2	9.10E-4	8.90E-4	2.25%
S3	0.15	20.18E-2	32.27E-4	32.72E-4	1.38%

2 Table2. Parameters  $\nu$  and  $h$  obtained with different sub-sequences

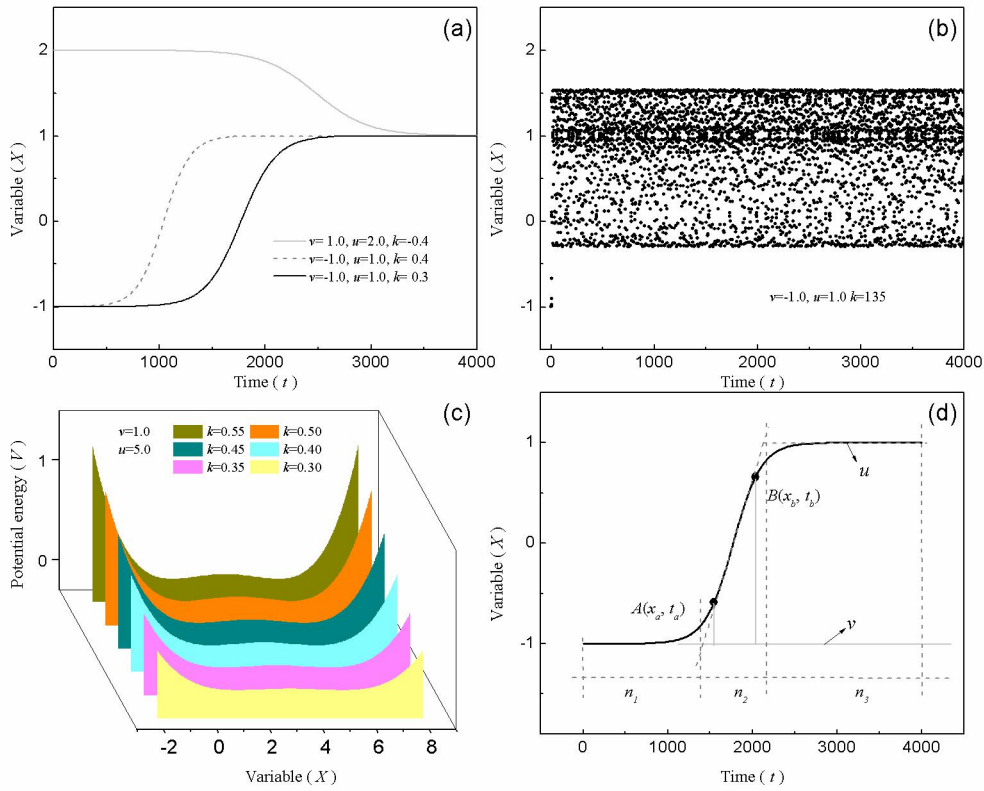
Length of sub-sequence	Start moment (year.month)	$\nu$	$h$ (month <sup>-1</sup> )
10a	2011.06	-0.45	1.054
20a	2011.06	-0.03	1.054
30a	2007.11	0.36	0.227
40a	2007.11	0.41	0.227

3



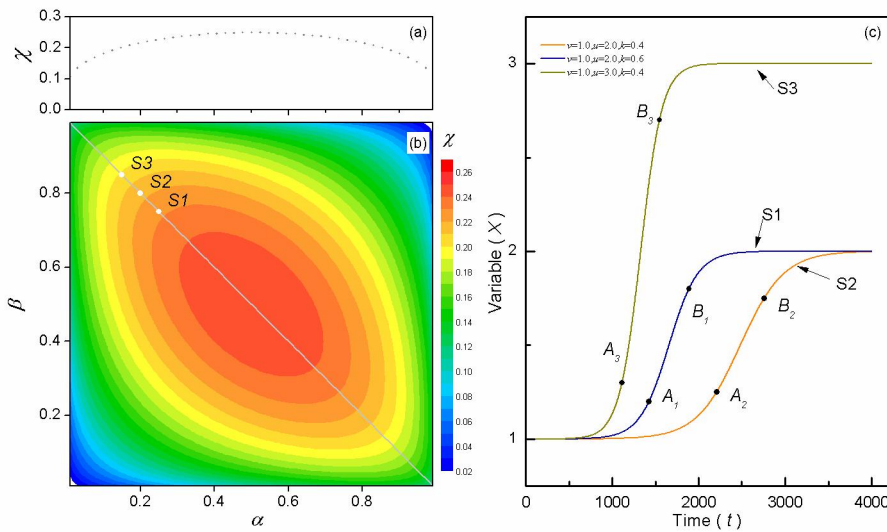
1

2 Figure 1. Transition process of abrupt change in real time sequence and  
 3 ideal time sequence. (a) The PDO time sequence during 1920 to 1970; (b) The PDO time  
 4 sequence during 1940 to 1945; (c) The transition process presented by piece-wise  
 5 function; (d) The transition process presented by continuous function.



1

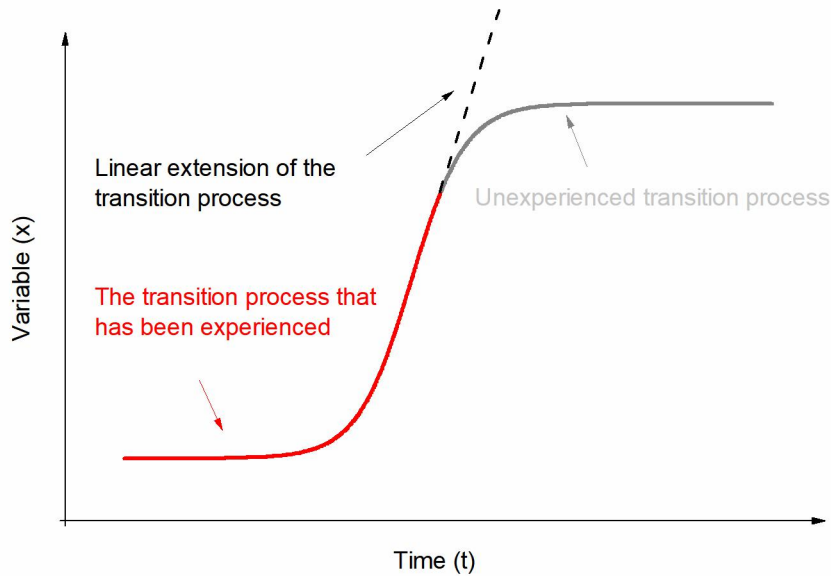
2 Figure 2. (a)The transition processes of system swinging between different stable  
 3 states since the parameters are different; (b)The system stays in unstable states; (c)The  
 4 generalized potential energy function of system performs differently since the  
 5 parameters are different; (d)Different segments of the transition process in the ideal  
 6 time sequence.



7

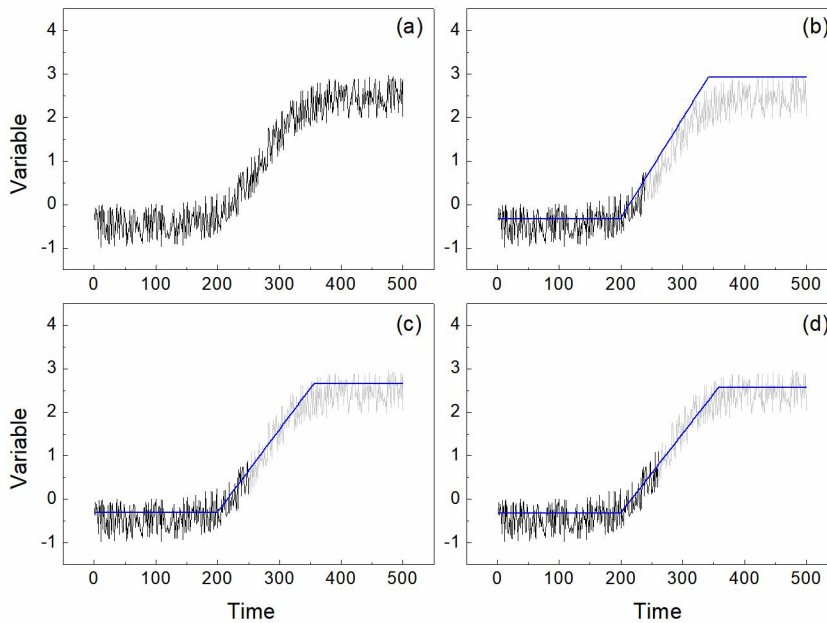
8 Figure 3. The relationship among the parameters  $\alpha$ ,  $\beta$ ,  $\chi$  and  $h$ . (a) Diagonal section of

- 1 parameter  $\chi$  in figure b (gray line);
- 2 (b) Parameter  $\chi$  with location parameters  $\alpha$  and  $\beta$ ;
- 3 (c) Points  $A$  and  $B$  stay in different positions in three situations marked as S1, S2, S3, and the dash lines connect the two points.



4

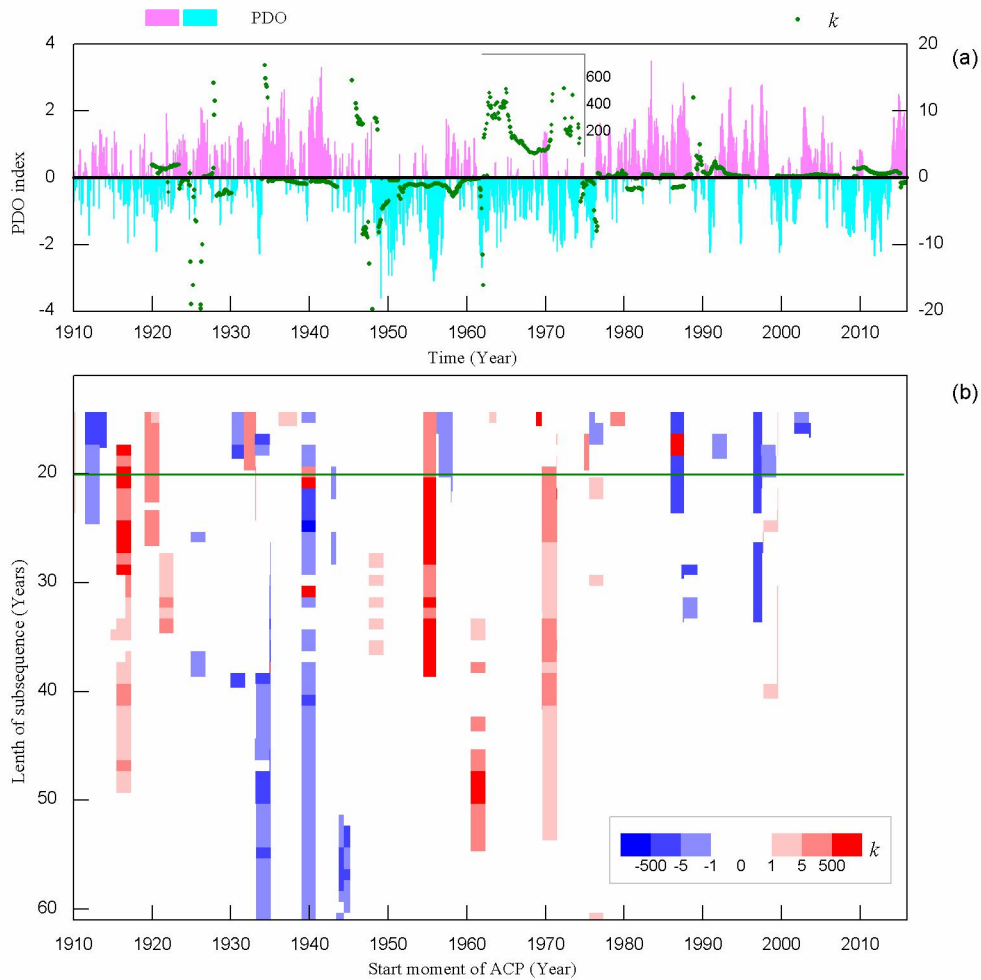
5 Figure 4. The schematic diagram of prediction method.



6

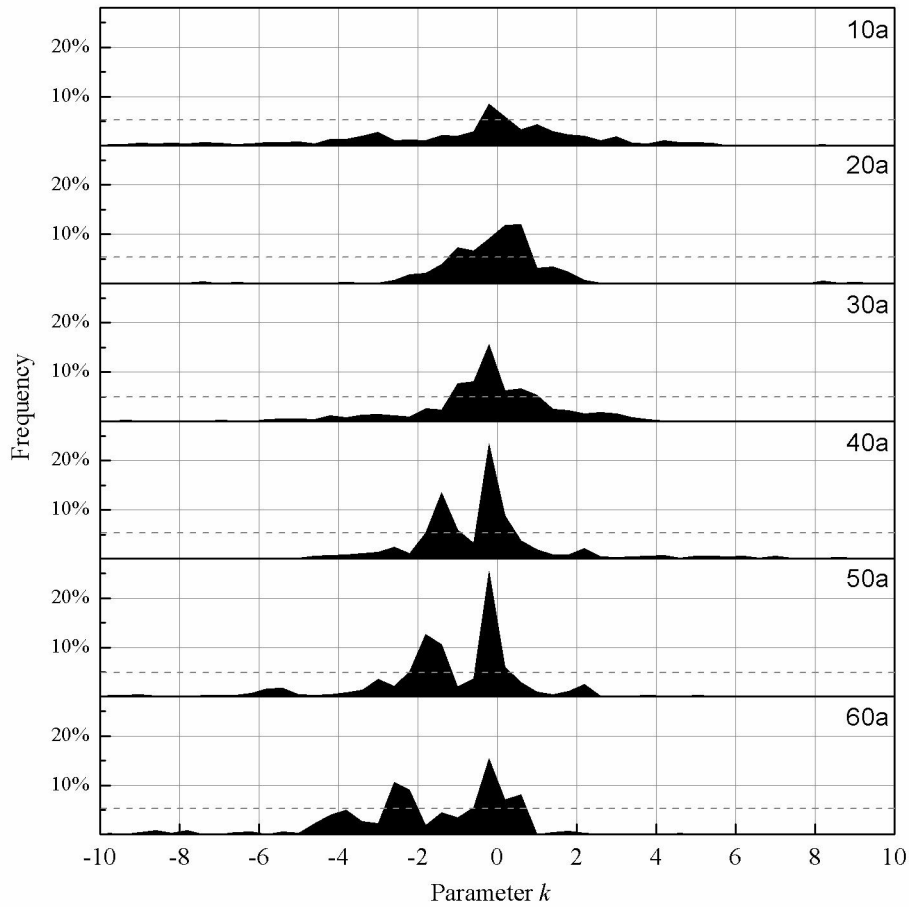
7 Figure 5. The ideal time sequence constructed by the logistic model and random  
 8 numbers. The X-axis represents time, and the Y-axis represents variable  $x_t$ . (a)  
 9 Completed transition process with 500 moments, Uncompleted transition processes  
 10 (the gray lines) and their prediction result (the blue lines) with (b) 240 moments, (c)

1 250 moments, and (d) 260 moments, the light gray lines are the original entire ideal  
 2 time sequences.



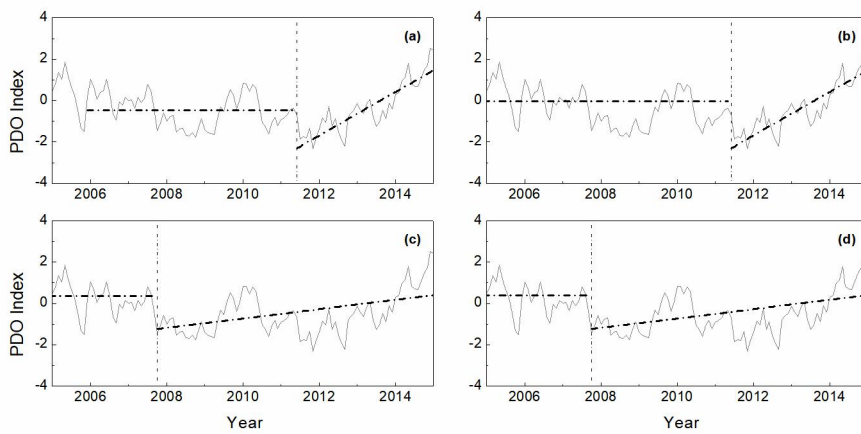
3

4 Figure 6. Identification of the PDO time sequence and instability parameter  $k$  with  
 5 different sub-sequence lengths. (a) The histogram represents the PDO time sequence  
 6 (left Y-axis), and the green dots indicate the value of parameter  $k$  when the  
 7 sub-sequence is 20 years (right Y-axis), where the X-axis represents time in year; (b)  
 8 the start moments of transition processes with different sub-sequence lengths (the red  
 9 color dots represent increasing processes, and blue color dots represent decreasing  
 10 changes, with deeper colors representing higher values). The green line represents that  
 11 the value of sub-sequence is 20 years. The X-axis represents the start moment of  
 12 abrupt change in year, and the Y-axis represents the sub-sequence length in years.



1

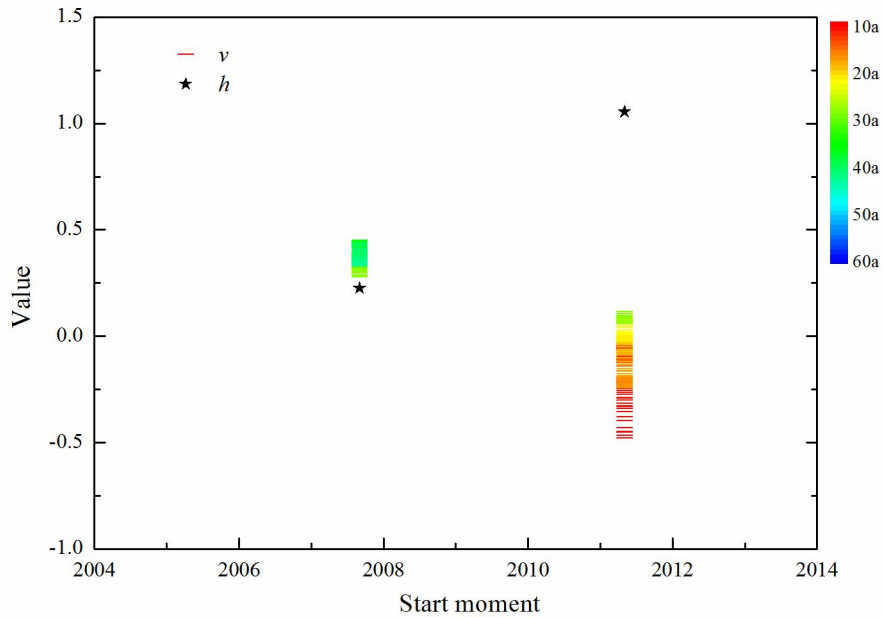
2 Figure 7. Statistical results of instability parameters for different sub-sequences  
 3 lengths. The X-axis is the value of parameter  $k$ , and the Y-axis is the statistical  
 4 frequency for the sub-sequence length of 10a, 20a 30a 40a 50a and 60a.



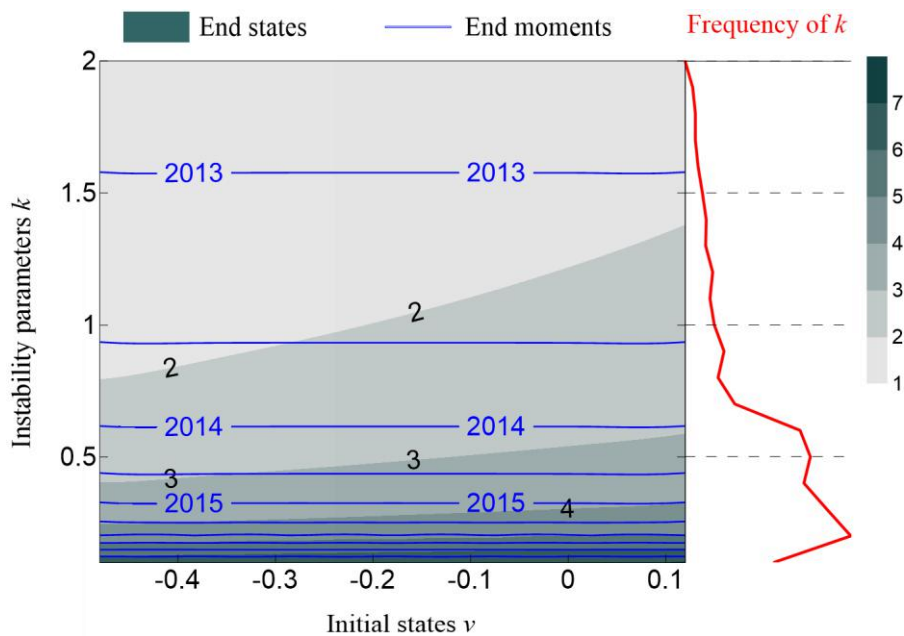
5

6 Figure 8. The PDO time sequences and the detection of parameters  $\nu$  and  $h$  when the  
 7 sub-sequence was set as (a)10 years, (b)20 years, (c)30 years, (d)40 years. The gray

- 1 lines represent the PDO time sequence. The horizontal dash lines represent initial
- 2 states, the slope dash lines represent linear trend lines of the transition process, and
- 3 vertical dotted lines represent the start moment.



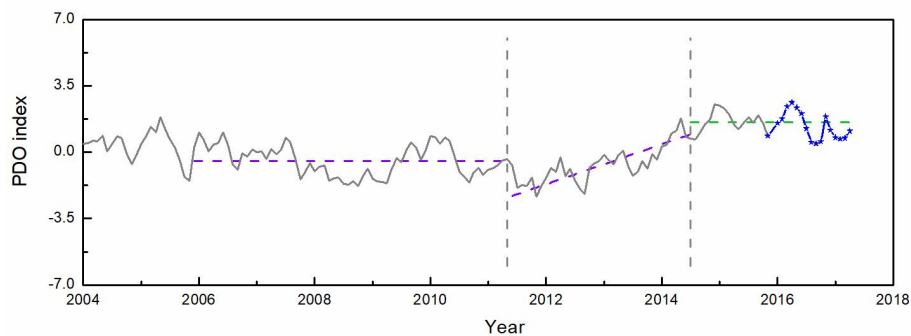
- 4
- 5 Figure 9. The values of the parameters  $v$  and  $k$  of two transition processes with
- 6 different lengths of sub-sequence. The black stars represent the values of parameter  $h$ ,
- 7 and the colourful short bar represent the values of parameter  $v$ . The colour bar
- 8 represents years of the sub-sequence length from 10 to 60 in intervals of 1.



9



1 Figure 10. Variation end state and end moment with the initial state parameter  $\nu$   
2 (horizontal ordinate) and instability parameter  $k$  (vertical coordinate). The red line on  
3 the right side shows the probability distribution of instability parameter  $k$ .



4

5 Figure 11. Prediction of the PDO index. The gray line represents the PDO index  
6 before 2015; the blue line represents the PDO index after 2015; the gray dash line  
7 represent the start moment and end moment; the purple dash lines represent the initial  
8 state and the linear trend line, the green line represent the prediction end state.

9